20th International Conference on Renewable Energies and Power Quality (ICREPQ'22)
Vigo (Spain), 27th to 29th July 2022
Renewable Energy and Power Quality Journal (RE&PQJ)
ISSN 2172-038 X, Volume No.20, September 2022

A Parametric Approach for the Study of Three-phase Inverters Subject to Grid Faults

A. Rolán[1] and L. Sainz[2]

[1] Department of Automatic Control
EEBE, Technical University of Catalonia (UPC)
Barcelona East School of Engineering – Av. Eduard Maristany 16, 08019, Barcelona (Spain)
Phone/Fax number: +0034 93 413 7360, e-mail: **alejandro.rolan@upc.edu**

[2] Department of Electrical Engineering
ETSEIB, Technical University of Catalonia (UPC)
Barcelona School of Industrial Engineering – Av. Diagonal 647, 08028, Barcelona (Spain)
Phone/Fax number: +0034 93 401 1759, e-mail: **luis.sainz@upc.edu**

Abstract. The aim of this work is to describe the behavior of three-phase inverters connected to a faulty grid by means of a parametric approach which gives rise to limaçon of Pascal curves and 3D figures formed by the injected currents during the fault. The analytical study is given in the complex form of the transformed *Park* variables, and the simulation results are obtained by means of MATLAB™. The results show that the parametric analysis can be an easy and useful tool to predict the behavior of three-phase inverters operating under voltage sags, with the aim of achieving fault ride-through (FRT) capability.

Key words. Fault ride-through (FRT) capability, inverter, power quality, renewable energy source (RES), voltage sag.

1. Introduction

During the last decades there has been a remarkable increase in the grid penetration of renewable energy sources (RESs). Truly, in 2020 there was a share of 29% of RESs in the electricity generation [1] and this share is expected to be 60% by 2050 [2]. Then, three-phase inverters will play an essential role in future power systems, since they are the link between RESs and the grid. As a result, studies on modeling and control of grid-connected inverters, powered by RESs, are needed in order to overcome grid disturbances [3].

Grid faults cause voltage sags (also known as dips), which are one of the most common grid disturbances [4]. They originate a decrease in the value of the rms voltage between 0.1 pu and 0.9 pu with respect to the pre-fault steady-state voltage, and the duration is between 1/2 cycle and 1 minute [5]. The most important trouble regarding voltage sags is the overcurrent that grid-connected equipment needs to withstand, which may produce, among other consequences, transformer saturation [6], pulsations in the DC link voltage [7] or torque peaks in induction machines [8]. Regarding grid-connected inverters operating under unbalanced voltage conditions, the most common approach is to use a dual current control (DCC) in order to control both *positive*- and *negative*-sequence currents [9]. Moreover, current grid codes may also be used in order to inject reactive current for voltage support during grid faults [10], [11].

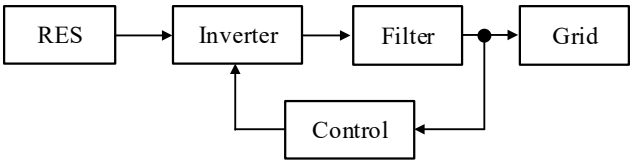

Fig. 1. Block diagram of a grid-connected inverter powered by a RES.

Analytical approaches are found in the technical literature in order to describe the behavior of three-phase inverters under a faulty grid [12]–[15]. This paper considers the author's previous work [16] regarding a geometric approach to predict the behavior of grid-connected inverters when operating under voltage sags, but it goes a step further: while [16] focuses the study in the complex plane, the present work analyzes the behavior in 3D. In order to do so, the limaçon of Pascal curve [17], which is formed by the locus of the injected current in the complex plane during voltage sags is analyzed in the three dimensions, and the behavior of this current is predicted accordingly for different fault durations. Then, this study provides a novel and easy approach to predict the behavior of the injected current by the inverter when operating under voltage sags, thus providing insights into fault ride-through (FRT) capability for grid-connected power converters.

2. Analytical Study

The block diagram of a grid-connected inverter is shown in Fig. 1. Assuming an RL filter and according to the generator-sign convention, the following electrical equation can be obtained:

$$\mathbf{v_i} = \mathbf{R}\mathbf{i} + (\mathrm{d}\mathbf{i}/\mathrm{d}t)\mathbf{L} + \mathbf{v_g} \quad (1)$$

where $\mathbf{v_i}$ is the vector with the per-phase inverter voltages (abc components), $\mathbf{v_g}$ is the vector with the per-phase grid voltages (abc components), $\mathbf{i}$ is the vector with the per-phase injected currents (abc components), and $\mathbf{R}$ and $\mathbf{L}$ are, respectively, the matrix with the per-phase filter's resistance and inductance (abc components).

Equation (1) can be written in the complex form of the transformed *Park* components as [12], [13]:

$$v_{\mathrm{if}} = [R + L(\mathrm{s} + \mathrm{j}\omega)]i_{\mathrm{f}} + v_{\mathrm{gf}}^{+} + v_{\mathrm{gf}}^{-}\mathrm{e}^{-\mathrm{j}2\omega t} \quad (2)$$

where s = d/dt, ω is the grid voltage pulsation, the superscripts + and – stand for the *positive*- and *negative*-sequence component, respectively, and the subscript f stands for the *forward* component of the transformed variable (which corresponds to the complex notation of the transformed *Park* variable, i.e: $\left(1/\sqrt{2}\right)\left(x_{\mathrm{d}} + \mathrm{j}x_{\mathrm{q}}\right)$, where x_{d} and x_{q} are the transformed *direct* and *quadrature* components, respectively, of the variable x). It should be noted that if v_{if} equals its steady-state value, then equation (2) is a first-order ODE with constant coefficients and its solution is [12], [13]:

$$i_{\mathrm{f}} = \frac{v_{\mathrm{if}} - v_{\mathrm{gf\,st}}}{R + \mathrm{j}\omega L} \quad ; \quad (t < t_{\mathrm{i}}) \quad (3)$$

$$i_{\mathrm{f}} = \underline{K}_1\,\mathrm{e}^{-(R/L)(t-t_{\mathrm{i}})}\,\mathrm{e}^{-\mathrm{j}\omega(t-t_{\mathrm{i}})} - \underline{K}_2\mathrm{e}^{-\mathrm{j}2\omega t} + \underline{K}_3 \quad ; \quad (t_{\mathrm{i}} \le t < t_{\mathrm{f}}) \quad (4)$$

$$i_{\mathrm{f}} = \underline{K}_4\,\mathrm{e}^{-(R/L)(t-t_{\mathrm{f}})}\,\mathrm{e}^{-\mathrm{j}\omega(t-t_{\mathrm{f}})} + \underline{K}_5 \quad ; \quad (t \ge t_{\mathrm{f}}) \quad (5)$$

where t_{i} is the time when the fault originates, t_{f} is the time when the fault is cleared, the subscript st stands for steady state and $\underline{K}_1$ … $\underline{K}_5$ are complex constants (see [12], [13] for more details).

In the author's previous work [16] a resemblance was noted between the transformed injected current during the fault event (4) and the limaçon of Pascal curve. The equation for this curve in polar coordinates is [17]:

$$r = b + a\cos(\theta) \quad (6)$$

where a is the circle radius, b is the conchoid's parameter and θ is the rotation angle, while in complex variables this curve is given by the following expression:

$$z = x + \mathrm{j}\,y = \frac{a}{2} + b\mathrm{e}^{\mathrm{j}\theta} + \frac{a}{2}\mathrm{e}^{\mathrm{j}2\theta} \quad . \quad (7)$$

As stated in [16], equation (4) can be expressed according to the following expression if the assumption of $R << L$ is done and if the time when the fault starts is set to $t_{\mathrm{i}} = 0$:

$$i_{\mathrm{f}} = \frac{\mathrm{j}}{X}\left[\left(v_{\mathrm{gf}}^{+} - v_{\mathrm{if}}\right) + \left(v_{\mathrm{gf\,st}} - v_{\mathrm{gf}}^{+} + v_{\mathrm{gf}}^{-}\right)\mathrm{e}^{-\mathrm{j}\omega t} - v_{\mathrm{gf}}^{-}\mathrm{e}^{-\mathrm{j}2\omega t}\right] \quad (8)$$

being X the filter reactance. Then, it is observed that (7) and (8) are equivalent expressions. As a result, a 2D analysis of the injected current by a three-phase inverter under voltage sags states that its shape corresponds to a limaçon of Pascal curve.

3. Simulation Results

A. System Parameters

The simulations have been carried out in MATLAB™. The analyzed three-phase inverter is connected to a grid with 50 Hz and 400 V (phase-to-phase). It is assumed that the inverter injects 50 kW (active power) to the grid under steady-state conditions and no reactive power is injected (unitary power factor). The RL filter has the following parameters: $R = 1$ mΩ and $L = 5$ mH. The per-unit (pu) values for voltages and currents are represented in this paper according to the following expressions:

$$v_{\mathrm{abc\,(pu)}} = \frac{v_{\mathrm{abc}}}{\sqrt{2}V_{\mathrm{N}}} \; ; \; i_{\mathrm{abc\,(pu)}} = \frac{i_{\mathrm{abc}}}{\sqrt{2}I_{\mathrm{N}}} \; ; \; i_{\mathrm{f\,(pu)}} = \frac{i_{\mathrm{f}}}{\sqrt{3/2}I_{\mathrm{N}}} \quad (9)$$

where V_{N} and I_{N} are the rated values of voltage and current, respectively.

B. Sag Type Influence

The following sag types have been simulated: A-type sag (caused by three-phase faults), C-type sag (caused by 2-phase faults) and F-type sag (caused by 2-phase-to-ground faults after a Dy transformer) [4]. The fault conditions have been simulated assuming a sag depth $h = 0.7$ (i.e., a voltage decrease of 30% with respect to the pre-fault steady-state conditions) and a duration $\Delta t = 100$ ms.

The results of the inverter operating under the aforementioned sags are shown in Fig. 2. The following two observations can be made according to these results. First, during symmetrical sags (A-type sags), the locus of the transformed injected current is a spiral that rotates at the pulsation of the grid voltages, as can be corroborated by the time evolution of the transformed injected current. Second, during unsymmetrical sags (B-type sag and F-type sag), the locus of the transformed injected current is not an spiral, but a limaçon of Pascal curve, as demonstrated by the comparison between equations (7) and (8). It should be noted that the term with twice the fundamental pulsation that appears in these equations is the reason why the initial spiral shape is transformed to the limaçon of Pascal curve. What is more, depending on the relationship between the coefficients a and b in (7) it leads to different locus shapes, such as the cardioid curve (which is obtained when $b = a$, shown in Fig. 2(b)) and a curve with an inner loop (which is obtained when $b < a$, shown in Fig. 2(c)). Note also that when $b = 0$, then the circle shape is obtained, as shown in Fig. 2(a).

C. 3D Representation

The locus of the real and imaginary parts of the transformed injected current, shown in the last row of Fig. 2, if plotted over time, give rise to the 3D representation shown in Fig. 3, where different sag durations have been simulated ($\Delta t = 100$ ms, 105 ms, 110 ms and 2 s). This representation is very useful because the behavior of three-phase inverters connected to a faulty grid under voltage sags can be easily predicted according to geometric figures. For example, let's take the case of symmetrical sags (A-type sag). According to Fig. 3 results, it could be stated that the 3D figure created by

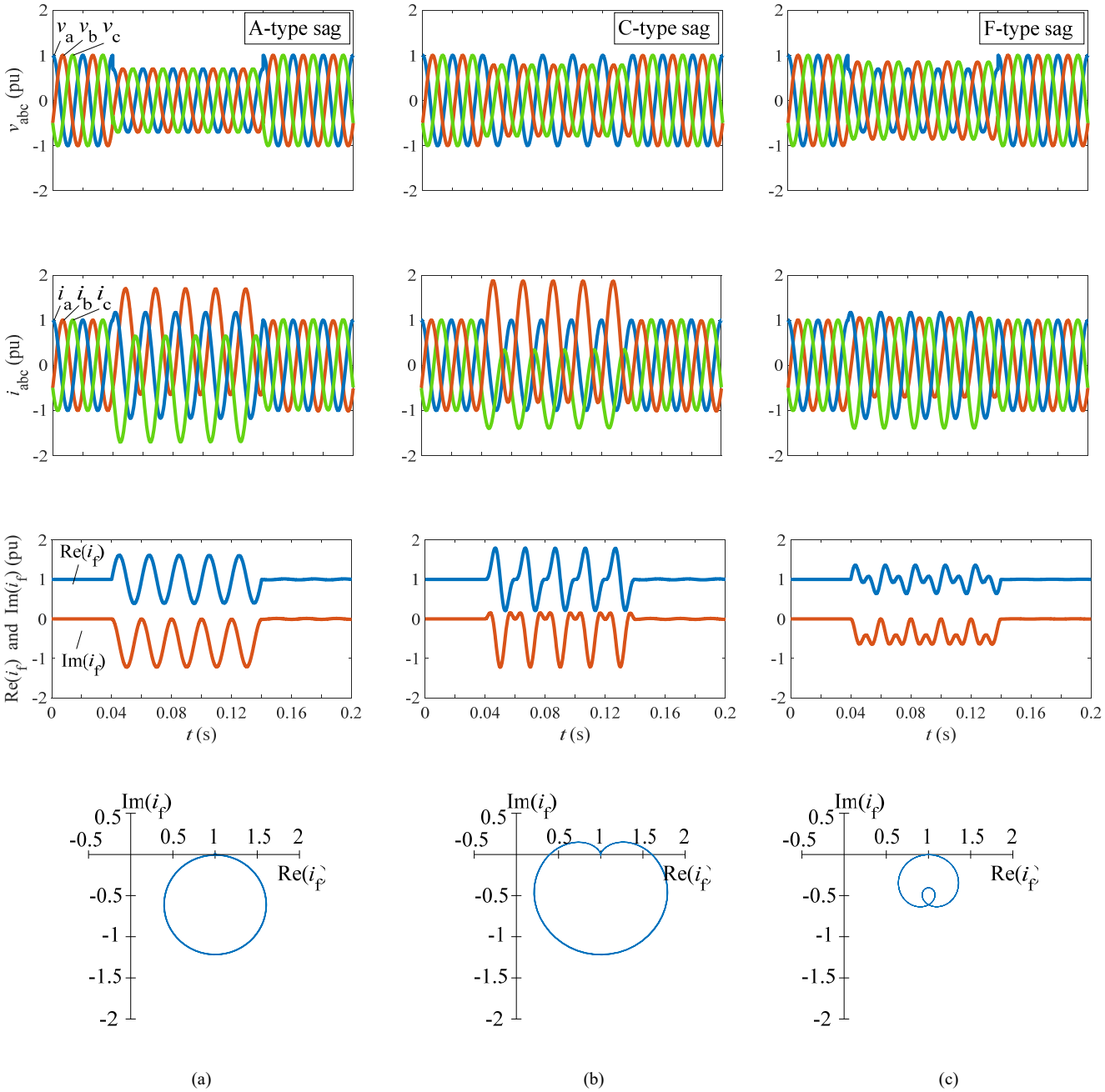

Fig. 2. Behavior of a three-phase inverter under voltage sags with depth $h = 0.7$ and duration $\Delta t = 100$ ms: time evolution of the abc voltages, time evolution of the abc injected currents and behaviour of the transformed injected currents (time evolution, locus and 3D plots). Inverter operating under (a) three-phase faults (A-type sag), (b) 2-phase faults (C-type sag), and (c) 2-phase-to-ground faults after a Dy transformer (F-type sag).

the combination of real and imaginary parts of the transformed currents during time corresponds to a cylinder. However, it should be noted that this is because the time constant is very high. Truly, note that $R = 1$ mΩ and $L = 5$ mH, so $\tau = L/R = 5$ s, which is the time constant of the system, so it will take $4\tau = 20$ s for the spiral to be closed. Note that this term appears in equation (4). The inverter's behavior can be exaggerated in order to show this damping effect on a 3D plot, for example by considering sags with very high durations, e.g. $\Delta t = 2$ s, as shown in the last row of Fig. 3.

D. Sag Duration Influence

It can be observed from the results shown in Fig. 3 that different sag durations give rise to different behavior after the fault. This is because the point on wave where the fault ends defines the behavior of the injected current after the sag. For example, if sag duration has n cycles, where $n = 1, 2, 3\ldots$ (e.g., $\Delta t = 100$ ms = 5 cycles (being $f = 50$ Hz)), then the locus of the injected current when the fault ends is located around its pre-fault steady-state value, so there is no rotation in the locus, as seen in the first row of Fig. 3, where there is almost a straight line, corresponding to the post-fault injected current. However, if sag duration has not an integer number of cycles, then when the fault ends (e.g. $\Delta t = 105$ ms = 5.25 cycles or $\Delta t = 110$ ms = 5.5 cycles), then the locus of the injected current is farther from its pre-fault steady-state value, so a larger path needs to be done in the locus of the injected current until reaching the steady state value, as shown in the second and the third row of Fig. 3, where a spiral shape appears in the locus of the injected current.

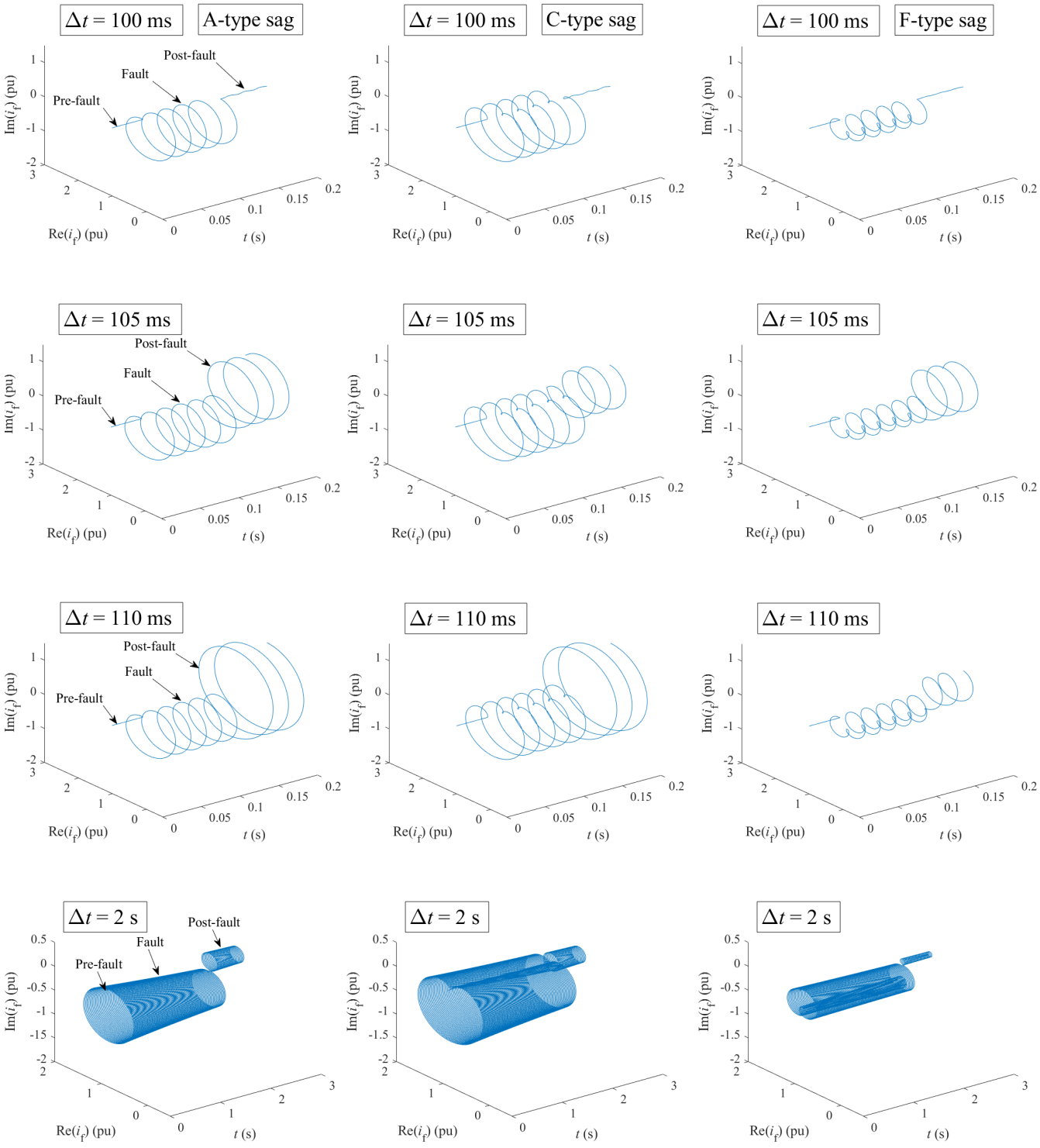

(a) (b) (c)

Fig. 3. 3D behavior of grid-connected inverters under voltage sags with depth h = 0.7 and durations Δt = 100 ms, 105 ms, 110ms and 2s: locus of the real and imaginary parts of the transformed injected current over time. Inverter operating under (a) three-phase faults (A-type sag), (b) 2-phase faults (C-type sag), and (c) 2-phase-to-ground faults after a Dy transformer (F-type sag).

E. Final Remarks

It has been shown that n number of cycles (n = 1, 2, 3…) in sag duration causes less severe effects on grid-connected inverters, since no large values of the injected current by the inverter appear after the fault event. However, non-integer number of cycles in sag duration causes the most severe effects on grid-connected inverters, because there appear large peak values in the injected current by the inverter.

4. Conclusion

This paper has shown a parametric approach to analyze the behavior of grid-connected inverters by means of a 3D

representation of the locus of real and imaginary parts of the transformed injected current over time. This approach can be used to easily predict the behavior of three-phase inverters when operating under both balanced or unbalanced fault conditions. It has been observed that sag durations with an integer number of cycles cause less severe effects on grid-connected inverters than sag durations with non-integer number of cycles. As a result, this paper has provided insights into fault ride-trough capability and the results could be used to develop more robust control strategies for grid-connected inverters operating under voltage sags.

Acknowledgement

This work has been supported in part by the Spanish Ministry of Science, Innovation and Universities under Grant RTI2018-095720-B-C33 and in part by Grant PID2020-112943RB-I00 funded by MCIN/AEI/10.13039/501100011033 from the Spanish Ministry of Science and Innovation. Prof. Alejandro Rolán would also like to thank Serra Húnter Program from the Government of Catalonia (Spain), from which he is a Fellow.

References

[1] Renewable Energy Policy Network for the 21st Century (REN21), Renewables 2021. Global status report, Paris, France (2021). Accessed: Mar. 04, 2022. [Online]. Available: http://www.ren21.net/

[2] Int. Renew. Energy Agency (IRENA), Global energy transformation. A roadmap to 2050, Abu Dhabi, UAE (2019). Accessed: Mar. 04, 2022. [Online]. Available: http://www.irena.org/

[3] R. Teodorescu, M. Liserre, and P. Rodríguez, Grid Converters for Photovoltaic and Wind Power Systems, Wiley-IEEE Press, Chichester, UK (2011).

[4] M. H. J. Bollen, Understanding Power Quality Problems: Voltage Sags and Interruptions, Wiley-IEEE Press, New York, USA (2000).

[5] IEEE Std. 1159–2019, IEEE Recommended Practice for Monitoring Electric Power Quality, 2019.

[6] L. Guasch, F. Córcoles, J. Pedra and L. Sáinz, "Effects of symmetrical voltage sags on three-phase three-legged transformers", IEEE Transactions on Power Delivery (2004). Vol. 19, no. 2, pp. 875-883.

[7] J. Pedra, F. Córcoles and F. J. Suelves, "Effects of balanced and unbalanced voltage sags on vsi-fed adjustable-speed drives", IEEE Transactions on Power Delivery (2005). Vol. 20, no. 1, pp. 224-233.

[8] L. Guasch, F. Córcoles and J. Pedra, "Effects of symmetrical and unsymmetrical voltage sags on induction machines", IEEE Transactions on Power Delivery (2004). Vol. 19, no. 2, pp. 774-782.

[9] H.-S. Song and K. Nam, "Dual current control scheme for pwm converter under unbalanced input voltage conditions", IEEE Transactions on Industrial Electronics (1999). Vol. 46, no. 5, pp. 953-959.

[10] A. Rolán, S. Bogarra and M. Bakkar, "Integration of distributed energy resources to unbalanced grids under voltage sags with grid code compliance", IEEE Transactions on Smart Grid (2022). Vol. 13, no. 1, pp. 355-366.

[11] M. Bakkar, S. Bogarra, A. Rolán, F. Córcoles and J. Saura, "Voltage sag influence on controlled three-phase grid-connected inverters according to the Spanish grid code", IET Generation, Transmission and Distribution (2020). Vol. 14, no. 10, pp. 1882-1892.

[12] A. Rolán, P. Giménez, S. J. Yagüe and S. Bogarra, "Modeling and control of a three-phase grid-connected inverter under fault conditions", in Proceedings of the International Symposium on Power Electronics, Electrical Drives, Automation and Motion (SPEEDAM), Amalfi, Italy (2018), pp. 479-484.

[13] A. Rolán, P. Giménez, S. J. Yagüe, S. Bogarra, J. Saura and M. Bakkar, "Voltage recovery influence on three-phase grid-connected inverters under voltage sags", IET Generation, Transmission and Distribution (2019). Vol. 13, no. 3, pp. 435-443.

[14] B. Mahamedi, M. Eskandari, J. E. Fletcher and J. Zhu, "Sequence-based control strategy with current limiting for the fault ride-through of inverter-interfaced distributed generators", IEEE Transactions on Sustainable Energy (2020). Vol. 11, no. 1, pp. 165-174.

[15] A. Camacho, M. Castilla, J. Miret, A. Borrell and L. García de Vicuña, "Active and reactive power strategies with peak current limitation for distributed generation inverters during unbalanced grid faults", IEEE Transactions in Industrial Electronics (2015). Vol. 62, no. 3, pp. 1515-1525.

[16] A. Rolán, "Behavior of three-phase inverters under grid faults explained from a geometric perspective", in Proceedings of the IEEE International Symposium on Industrial Electronics (ISIE), Kyoto, Japan (2021), pp. 1-6.

[17] J. D. Lawrence, A Catalog of Special Plane Curves, Dover Publications Inc., New York, USA (2014), pp. 113-117.